

Foil Winding Resistance and Power Loss in Individual Layers of Inductors

Marian K. Kazimierczuk and Rafal P. Wojda

Abstract—This paper presents an estimation of high-frequency winding resistance and power loss in individual inductor layers made of foil, taking into account the skin and proximity effects. Approximated equations for power loss in each layer are given and the optimal values of foil thickness for each layer are derived. It is shown that the winding resistance of individual layers significantly increases with the operating frequency and the layer number, counting from the center of an inductor. The winding resistance of each foil layer exhibits a minimum value at an optimal layer thickness. The total winding resistance increases with the total number of layers.

Keywords—Eddy currents, individual layer winding resistance, inductors, optimal foil thickness, proximity effect, skin effect, winding power loss.

I. INTRODUCTION

GENERALLY, the power loss in the winding of an inductor at high frequencies is caused by two effects of eddy currents: skin effect and the proximity effect [3]-[17], [5]-[8], [10]-[20]. These effects influence the distribution of the current in the conductor, causing an increase in the winding resistance. Moreover, the winding resistance and the winding power loss increase with the operating frequency. The skin effect is caused in the conductor by the magnetic field induced by its own current. The skin effect is identical in all layers. The proximity effect is caused by the magnetic field induced by currents flowing in the adjacent conductors. The proximity effect increases rapidly when the layer number increases. Inductors made of copper foil have beneficial properties in designing power circuits. Its thermal, mechanical, and electrical properties are much better than the properties of round wire inductors. Foil winding are attractive in low profile inductors and transformers. In addition, they are commonly used in high current magnetic components.

The purpose of this paper is to present the analysis of winding resistance of individual layers in multilayer foil inductors with a magnetic core and compare their properties with those of the uniform layer thickness.

II. GENERAL EQUATION FOR RESISTANCE OF INDIVIDUAL LAYERS

Inductors made up of straight, parallel foil conductor are considered. There is one winding turn in each layer. This model can be used for low profile flat inductors and inductors

This work was supported by the Fulbright Foundation.

M. K. Kazimierczuk and R. P. Wojda are with the Department of Electrical Engineering, Wright State University, 3640 Colonel Glenn Highway, Dayton, Ohio, 45435, USA (e-mail: marian.kazimierczuk@wright.edu; wojda.2@wright.edu).

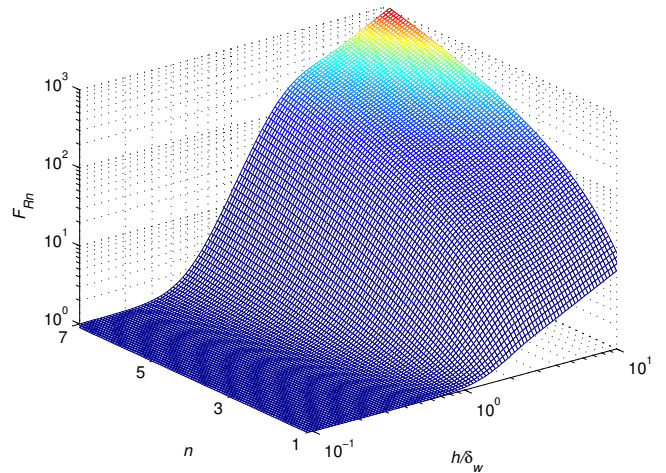


Fig. 1. 3-D plot of ac-to-dc resistance ratio F_{Rn} as a function of h/δ_w and n .

wound on round magnetic cores with low radius of curvature. The magnetic field H in this kind of inductors can be described by the second-order ordinary differential equation, called the Helmholtz equation,

$$\frac{d^2 H}{dx^2} = \gamma^2 H, \quad (1)$$

where γ is the complex propagation constant described by

$$\gamma = \sqrt{j\omega\mu_0\sigma_w} = \sqrt{\frac{j\omega\mu_0}{\rho_w}} = \frac{\sqrt{2j}}{\rho_w} = \frac{1+j}{\rho_w}, \quad (2)$$

the skin depth is

$$\delta_w = \sqrt{\omega\mu_0\sigma_w} = \frac{1}{\sqrt{\pi f\mu_0\sigma_w}} = \frac{\rho_w}{\pi f\mu_0}, \quad (3)$$

$\rho_w = 1/\sigma_w$ is the conductor resistivity, f is the operating frequency, and μ_0 is the free space permeability. The solution of (1) leads to the distribution of the magnetic field intensity H and the current density J in the n -th winding layer. The complex power in the n -th layer is [18]

$$P_{wn} = \frac{\rho_w l_T I_m^2 \gamma}{2b} \left[\coth(\gamma h) + 2(n^2 - n) \tan\left(\frac{\gamma h}{2}\right) \right], \quad (4)$$

where h is the thickness of foil, b is the breadth of the foil and l_T is the mean turn length (MTL). Assume that the current flowing through the inductor foil winding is sinusoidal

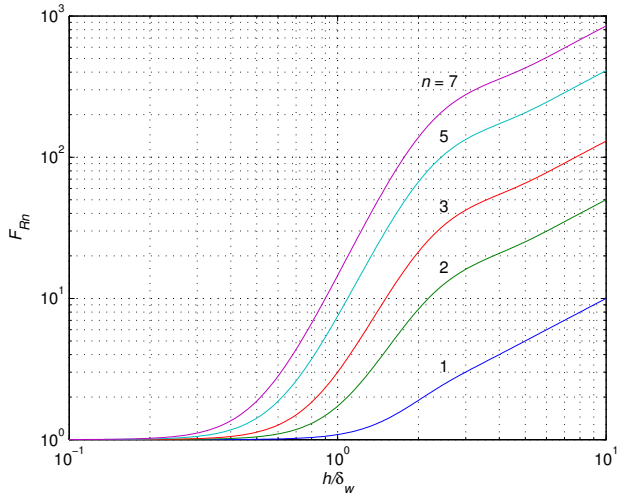


Fig. 2. Individual layers ac-to-dc resistance ratio F_{Rn} as a function of h/δ_w for each of the first several layers.

$$i_L = I_m \sin(\omega t). \quad (5)$$

The time-average real power loss in the n -th layer is

$$P_{wn} = R_{wn} I_{rms}^2 = [R_{skin(n)} + R_{prox(n)}] I_{rms}^2 = [R_{skin} + R_{prox(n)}] I_{rms}^2, \quad (6)$$

where $R_{skin(n)} = R_{skin}$ is the resistance of each layer due to the skin effect and is the same for each layer and $R_{prox(n)}$ is the resistance of the n -th layer due to the proximity effect and appreciably increases from the innermost layer to the outermost layer. If the RMS current is equal to the dc current through the inductor, then the time-average real power loss in the n -th layer of the winding P_{wn} , normalized with respect to the dc power loss P_{wdcn} , is equal to the ac-to-dc resistance ratio of the n -th layer R_{wn}/R_{dcn} . Hence, the ac-to-dc resistance ratio in the n -th layer is given by [1]

$$F_{Rn} = \frac{P_{wn}}{P_{wdcn}} = \frac{R_{wn}}{R_{wdcn}} = \left(\frac{h}{\delta_w} \right) \left[(2n^2 - 2n + 1) \frac{\sinh(\frac{2h}{\delta_w}) + \sin(\frac{2h}{\delta_w})}{\cosh(\frac{2h}{\delta_w}) - \cos(\frac{2h}{\delta_w})} - 4(n^2 - n) \frac{\sinh(\frac{h}{\delta_w}) \cos(\frac{h}{\delta_w}) + \cosh(\frac{h}{\delta_w}) \sin(\frac{h}{\delta_w})}{\cosh(\frac{2h}{\delta_w}) - \cos(\frac{2h}{\delta_w})} \right]. \quad (7)$$

Fig. 1 shows a 3-D plot of ac resistance ratio F_{Rn} as a function of h/δ_w and n . Fig. 2 shows plots of F_{Rn} as a function of h/δ_w for several individual layers. It can be seen that the normalized ac-to-dc resistance ratio F_{Rn} significantly increases as the ratio h/δ_w increases and as the layer number n increases, counting from the innermost layer to the outermost layer. At a fixed foil thickness h , three frequency ranges can be distinguished: low-frequency range, medium-frequency range, and high-frequency range. In the low-frequency range, $h \ll 2\delta_w$, the skin and the proximity effects are negligible, the current density is uniform, $R_w \approx R_{wdc}$, and therefore

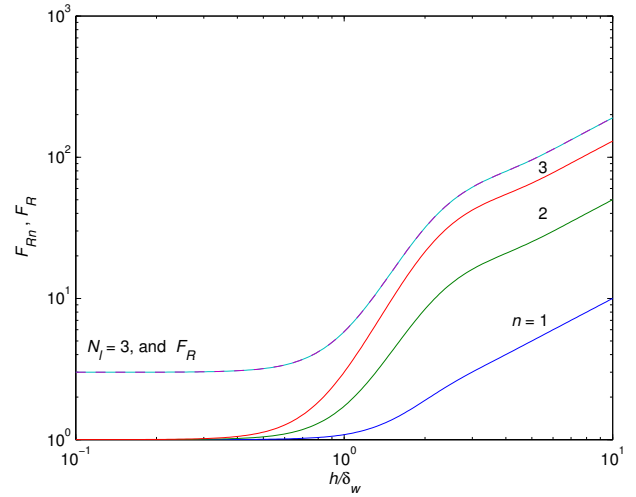


Fig. 3. Plots of F_{Rn} and F_R as a function of h/δ_w for three layer foil winding inductor ($N_l = 3$) and for total resistance of three layers.

$F_{Rn} \approx 1$. In the medium-frequency range, the current density is no longer uniform, and thereby F_{Rn} increases with frequency. The boundary between the low and medium frequency ranges decreases as the layer number n increases. In the high-frequency range, the current flows only near both foil surfaces and F_{Rn} increases with frequency. The rate of increase of F_{Rn} in the high-frequency range is lower than that in the-medium frequency range for $n \geq 2$. The sum of the ac-to-dc resistance ratios of all layers is given by

$$F_{RNS} = \frac{R_{w1}}{R_{wdc1}} + \frac{R_{w2}}{R_{wdc2}} + \frac{R_{w3}}{R_{wdc3}} \dots \frac{R_{wN_l}}{R_{wdcN_l}} = \sum_{n=1}^{N_l} F_{Rn}. \quad (8)$$

where N_l is the number of foil winding layers. Fig. 3 shows plots of F_{Rn} and F_{RNS} as functions of h/δ_w for three-layer foil winding inductor.

The ac-to-dc resistance ratio F_{Rn} can be expressed as

$$F_{Rn} = F_S + F_{Pn}, \quad (9)$$

where the skin effect ac-to-dc resistance ratio is identical for each layer and is expressed by

$$F_S = \frac{R_{skin}}{R_{wdcn}} = \left(\frac{h}{\delta_w} \right) \frac{\sinh(\frac{2h}{\delta_w}) + \sin(\frac{2h}{\delta_w})}{\cosh(\frac{2h}{\delta_w}) - \cos(\frac{2h}{\delta_w})} \quad (10)$$

and the proximity effect ac-to-dc resistance ratio of the n -th layer is given by

$$F_{Pn} = \frac{R_{prox(n)}}{R_{wdcn}} = 2n(n-1) \left(\frac{h}{\delta_w} \right) \frac{\sinh(\frac{h}{\delta_w}) - \sin(\frac{h}{\delta_w})}{\cosh(\frac{h}{\delta_w}) + \cos(\frac{2h}{\delta_w})}. \quad (11)$$

The skin effect factor F_S is identical for all the winding layers. The proximity effect factor F_{Pn} is zero for the first layer and rapidly increases with the layer number n . For multilayer inductors, the proximity effect becomes dominant. Fig. 4 shows the skin effect factor F_S as a function of h/δ_w for each layer. It can be seen that the skin effect is negligible for $h/\delta_w < 1$. For $h/\delta_w > 1$, F_S increases rapidly with h/δ_w . The

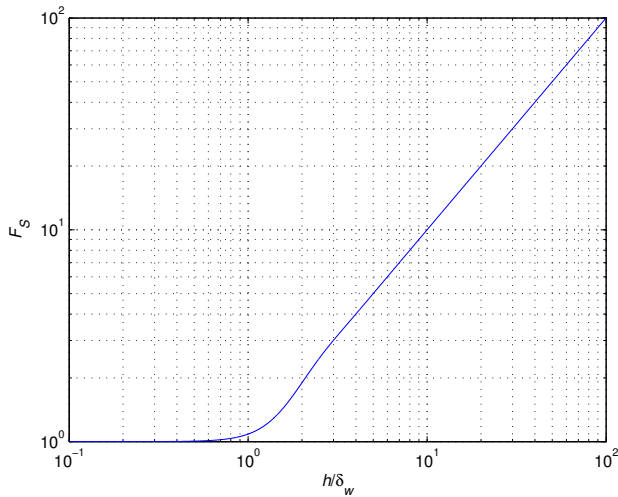


Fig. 4. Skin effect factor F_S as a function h/δ_w for each layer.

proximity effect factor F_{Pn} as a function of h/δ_w is shown in Figs. 5 and 6 in linear-log and log-log scales, respectively. It can be seen from Fig. 5 that the proximity effect is negligible for $h/\delta_w < 1$ and does not exist for the first layer. It can be observed from Fig. 6 that the proximity effect factor F_{Pn} increases rapidly with h/δ_w for the range $1 < h/\delta_w < 2$ and increases with h/δ_w at a lower rate for $h/\delta_w > 2$.

III. OPTIMUM THICKNESS OF INDIVIDUAL LAYERS

The effective width of the current flow is approximately equal to the skin depth δ_w . Therefore, the winding resistance and the power loss in the innermost layer at high frequencies are, respectively,

$$R_{w1(HF)} = \frac{\rho_w l_T}{b \delta_w} \quad (12)$$

and

$$P_{w1(HF)} = \frac{\rho_w l_T I_{Lm}^2}{2b \delta_w}. \quad (13)$$

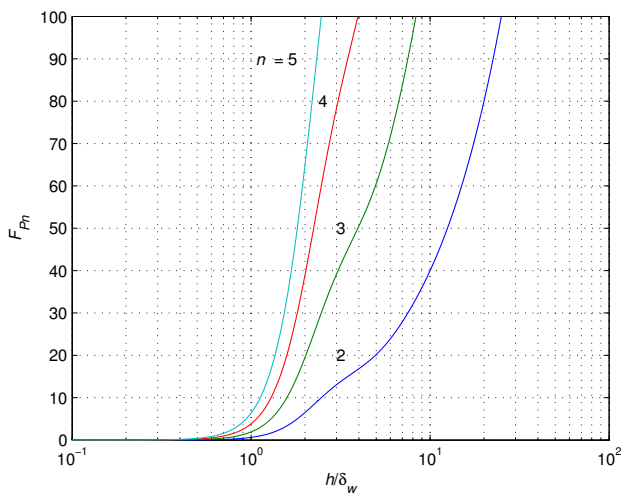


Fig. 5. Proximity effect factor F_{Pn} as a function h/δ_w for n -th layer in linear-log scale.

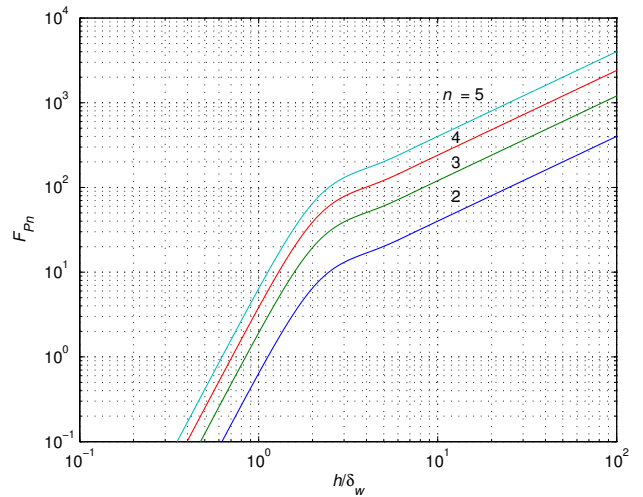


Fig. 6. Proximity effect factor F_{Pn} as a function h/δ_w for n -th layer in log-log scale.

The dc resistance of a single layer is

$$R_{wdc1} = \frac{\rho_w l_T}{hb}. \quad (14)$$

The normalized winding resistance of the n -th layer is

$$\begin{aligned} F_{rn} &= \frac{R_{wn}}{\frac{\rho_w l_T}{b \delta_w}} = \frac{R_{wn}}{R_{w1(HF)}} = \frac{F_{Rn}}{\frac{h}{\delta_w}} \\ &= (2n^2 - 2n + 1) \frac{\sinh(\frac{2h}{\delta_w}) + \sin(\frac{2h}{\delta_w})}{\cosh(\frac{2h}{\delta_w}) - \cos(\frac{2h}{\delta_w})} \\ &\quad - 4(n^2 - n) \frac{\sinh(\frac{h}{\delta_w}) \cos(\frac{h}{\delta_w}) + \cosh(\frac{h}{\delta_w}) \sin(\frac{h}{\delta_w})}{\cosh(\frac{2h}{\delta_w}) - \cos(\frac{2h}{\delta_w})}. \end{aligned} \quad (15)$$

Fig. 7 shows a 3-D plot of normalized ac resistance $R_{wn}/(\rho_w l_T/b \delta_w)$ as a function of h/δ_w and n . Fig. 8 shows plots of $R_{wn}/(\rho_w l_T/b \delta_w)$ as a function of h/δ_w for several

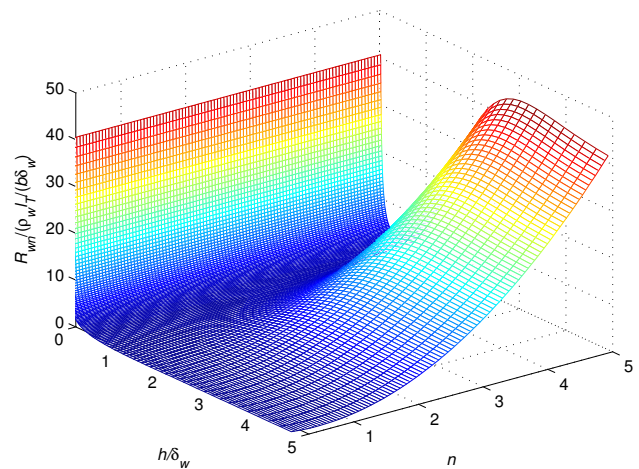


Fig. 7. 3-D plot of normalized ac resistance $R_{wn}/(\rho_w l_T/b \delta_w)$ as a function of h/δ_w and n .

individual layers. It can be seen that the ac resistance reaches a fixed value at higher values of h/δ_w . It can be also seen that the plots exhibit minimum values. Fig. 9 shows these plots in the vicinity of the minimum values in more detail.

IV. APPROXIMATION OF $R_{wn}/R_{w1(HF)}$

An exact analytical expression for the minimum winding resistance of individual layers cannot be found from (15). For low and medium foil thicknesses, the winding resistance of the first layer, (15) can be approximated by

$$F_{rn} = \frac{R_{wn}}{\frac{\rho_w l_T}{b \delta_w}} = \frac{R_{wn}}{R_{w1(HF)}} = \frac{P_{wn}}{P_{w1(HF)}} \approx \frac{1}{\frac{h}{\delta_w}} \text{ for } \frac{h}{\delta_w} < 1 \text{ and } n = 1 \quad (16)$$

and for large foil thicknesses,

$$F_{rn} = \frac{R_{wn}}{\frac{\rho_w l_T}{b \delta_w}} = \frac{R_{wn}}{R_{w1(HF)}} = \frac{P_{wn}}{P_{w1(HF)}} \approx 1 \text{ for } \frac{h}{\delta_w} > 1 \text{ and } n = 1. \quad (17)$$

Fig. 10 shows the exact and approximate plots of $R_{w1}/(\rho_w l_T/b\delta_w)$ as functions of h/δ_w for the first layer. For low and medium foil thicknesses, the normalized winding resistance and normalized winding power loss in the n -th layer can be approximated by

$$F_{rn} = \frac{R_{wn}}{\frac{\rho_w l_T}{b \delta_w}} = \frac{R_{wn}}{R_{w1(HF)}} = \frac{P_{wn}}{P_{w1(HF)}} \approx \frac{1}{\frac{h}{\delta_w}} + \frac{n(n-1)}{3} \left(\frac{h}{\delta_w} \right)^3 \text{ for } \frac{h}{\delta_w} < 1.5 \text{ and } n \geq 2 \quad (18)$$

or

$$F_{Rn} = \frac{R_{wn}}{R_{wdc1}} = \frac{P_{wn}}{P_{wdc1}}$$

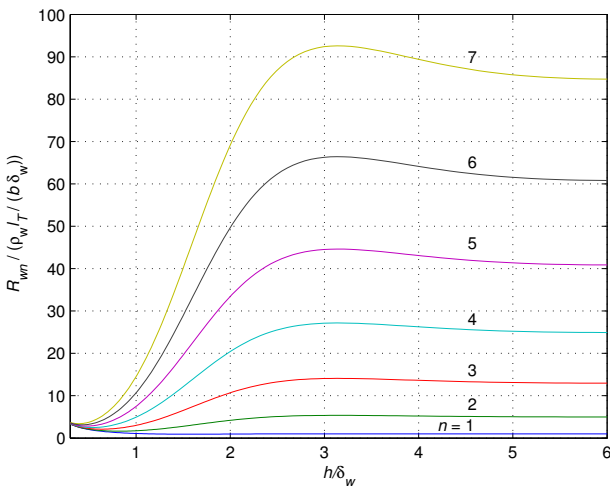


Fig. 8. Normalized ac resistance $R_{wn}/(\rho_w l_T/b\delta_w)$ as a function of h/δ_w for each of the first several layers.

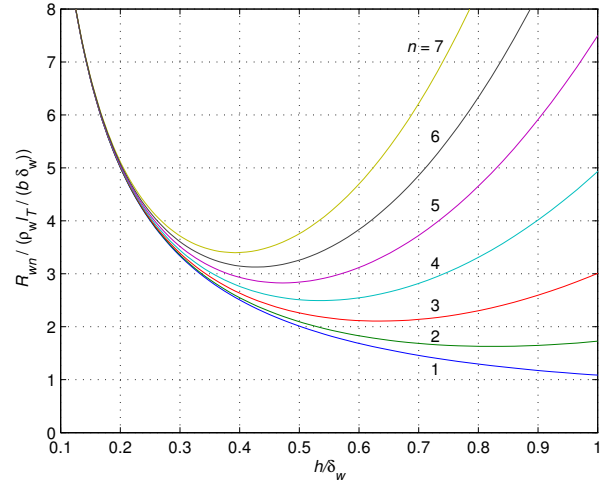


Fig. 9. Normalized ac resistance $R_{wn}/(\rho_w l_T/b\delta_w)$ as a function of h/δ_w for each of the first several layers in enlarged scale.

$$\approx 1 + \frac{n(n-1)}{3} \left(\frac{h}{\delta_w} \right)^4 \text{ for } \frac{h}{\delta_w} < 1.5 \text{ and } n \geq 2. \quad (19)$$

Fig. 11 shows exact and approximate plots of $R_{w3}/(\rho_w l_T/b\delta_w)$ as functions of h/δ_w at $n = 3$ for low and medium foil thicknesses. It can be seen that the approximation is excellent in vicinity of the minimum value of the layer resistance. For high thickness of the foil, the normalized winding resistance and normalized winding power loss in the n -th layer is approximately given by

$$F_{rn} = \frac{R_{wn}}{R_{w1(HF)}} = \frac{P_{wn}}{P_{w1(HF)}}$$

$$\approx n^2 + (n-1)^2 \text{ for } 5 \leq \frac{h}{\delta_w} \leq \infty \quad (20)$$

or

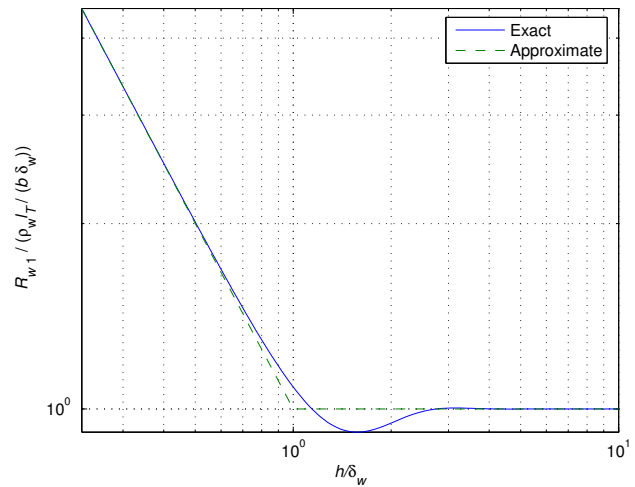


Fig. 10. Exact and approximated plots of $R_{w1}/(\rho_w l_T/b\delta_w)$ as a function of h/δ_w for $n=1$.

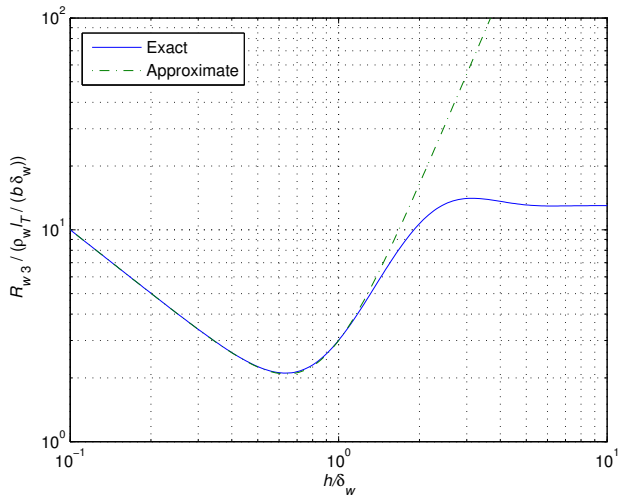


Fig. 11. Exact and approximate plots of $R_{w3}/(\rho_w l_T/b\delta_w)$ as functions of h/δ_w at $n = 3$ for low and medium thickness.

$$F_{Rn} = \frac{R_{wn}}{R_{wdc1}} = \frac{P_{wn}}{P_{wdc1}} \approx \left(\frac{h}{\delta_w}\right) [n^2 + (n-1)^2] \text{ for } 5 \leq \frac{h}{\delta_w} \leq \infty. \quad (21)$$

Fig. 12 shows exact and approximate plots of $R_{w3}/(\rho_w l_T/b\delta_w)$ as functions of h/δ_w at $n = 3$ for high foil thicknesses.

Taking the derivative of (7) with respect to h/δ_w , we obtain

$$\cos\left(\frac{h}{\delta_w}\right) = \frac{n-1}{n} \cosh\left(\frac{h}{\delta_w}\right). \quad (22)$$

For $n = 1$, (22) becomes

$$\cos\left(\frac{h}{\delta_w}\right) = 0, \quad (23)$$

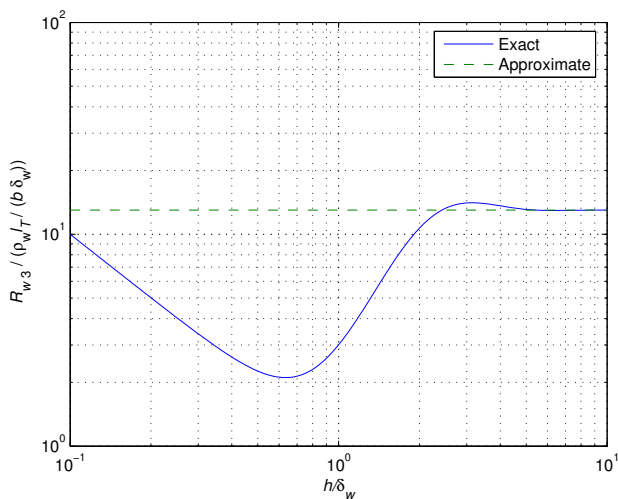


Fig. 12. Exact and approximate plots of $R_{w3}/(\rho_w l_T/b\delta_w)$ as functions of h/δ_w at $n = 3$ for high thickness.

TABLE I
EXACT AND APPROXIMATE OPTIMUM FOIL THICKNESS FOR INDIVIDUAL INDUCTOR LAYERS

Layer Number	Exact	Approximate
n	h_{optn}/δ_w	h_{optn}/δ_w
1	$\pi/2$	1.5707
2	0.823767	0.8409
3	0.634444	0.6389
4	0.535375	0.5373
5	0.471858	0.4729
6	0.426676	0.4273
7	0.392413	0.3928
8	0.365274	0.3656
9	0.343089	0.3433
10	0.324512	0.3247

which gives the optimum thickness of the first layer, subjected only to the skin effect

$$\frac{h_{opt1}}{\delta_w} = \frac{\pi}{2} \text{ for } n = 1. \quad (24)$$

For $n \geq 2$, (22) has no closed-form solution and was solved numerically; the exact results are given in Table I. In order to obtain analytical expression for h_{opt}/δ_w , we will use (18). The minimum values of the ac resistance $R_{wn(min)}$ and the winding power loss $P_{wn(min)}$ in the n -th layer for $n \geq 2$ are obtained by taking the derivative of (18) and setting the result to zero

$$\frac{d\left(\frac{R_{wn}}{R_{w1(HF)}}\right)}{d\left(\frac{h}{\delta_w}\right)} = \frac{-1}{\left(\frac{h}{\delta_w}\right)^2} + \left(\frac{h}{\delta_w}\right)^2 n(n-1) = 0, \quad (25)$$

yielding the optimum thickness of the n -th layer

$$\frac{h_{optn}}{\delta_w} = \frac{1}{\sqrt[4]{n(n-1)}} \text{ for } n \geq 2. \quad (26)$$

The approximated results of h_{optn}/δ_w , are listed in Table I.

The minimum normalized power loss in the n -th layer is

$$\frac{R_{wn(min)}}{R_{w1(HF)}} = \frac{P_{wn(min)}}{P_{w1(HF)}} = \frac{4}{3} \sqrt[4]{n(n-1)} \text{ for } n \geq 2. \quad (27)$$

Dividing (26) by (24), one obtains the ratio of the optimum thickness of the n -th layer to the optimum thickness of the first layer as

$$\frac{h_{optn}}{h_{opt1}} = \frac{2}{\pi \sqrt[4]{n(n-1)}} \text{ for } n \geq 2. \quad (28)$$

V. EXAMPLE FOR OPTIMUM WINDING RESISTANCE

The minimum winding resistance can be achieved when the thickness of each layer is different and equal to the optimum value given by (24) and (26). For three-layer copper inductor and conducting sinusoidal current at frequency 43 kHz, the optimum thickness of the bare foil of the first layer is

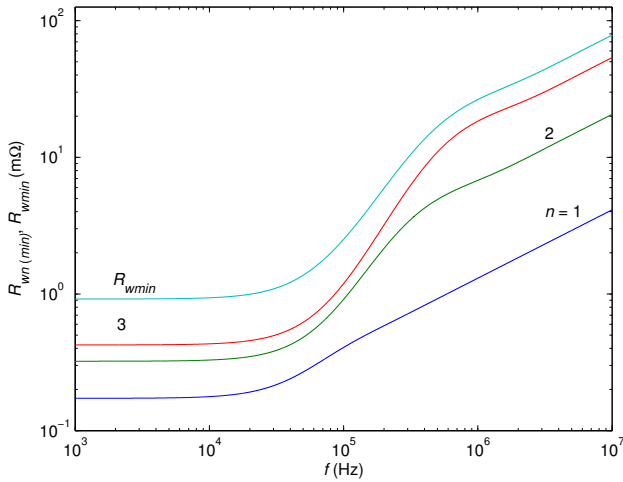


Fig. 13. Plots of $R_{wn(min)}$ and R_{wmin} as a function of frequency f for the foil inductor.

$$h_{opt1} = \frac{\pi}{2} \delta_w = \frac{\pi}{2} \sqrt{\frac{\rho_w}{\pi f \mu_0}} \approx 0.5 \text{ mm}. \quad (29)$$

From (28), the optimum thickness of the bare conductor of the second layer $n = 2$ is

$$h_{opt2} = \frac{2}{\pi \sqrt[4]{2}} h_{opt1} = 0.5356 \times 0.5 = 0.267 \text{ mm}, \quad (30)$$

and the optimum thickness of the bare conductor of the third layer $n = 3$ is

$$h_{opt3} = \frac{2}{\pi \sqrt[4]{6}} h_{opt1} = 0.406 \times 0.5 = 0.203 \text{ mm}. \quad (31)$$

The ac winding resistance for n -th layer is given by

$$R_{wn} = F_{Rn} R_{wdcn}. \quad (32)$$

Therefore, the overall ac resistance of the foil inductor is

$$R_w = \sum_{n=1}^{N_l} F_{Rn} R_{wdcn}. \quad (33)$$

The breadth of the inductor, which is equal to the foil width is $b = 2 \text{ cm}$. The length of each turn is $l_T = 10 \text{ cm}$. The resistivity of copper at room temperature is $\rho_{Cu} = 1.72 \times 10^{-8} \Omega\text{m}$. The dc resistances of each layer is

$$R_{wdc1} = \frac{\rho_{Cu} l_T}{b h_{opt1}} = \frac{1.72 \times 10^{-8} \times 0.1}{0.5 \times 10^{-3} \times 20 \times 10^{-3}} = 0.172 \text{ m}\Omega, \quad (34)$$

$$R_{wdc2} = \frac{\rho_{Cu} l_T}{b h_{opt2}} = \frac{1.72 \times 10^{-8} \times 0.1}{0.267 \times 10^{-3} \times 20 \times 10^{-3}} = 0.322 \text{ m}\Omega, \quad (35)$$

$$R_{wdc3} = \frac{\rho_{Cu} l_T}{b h_{opt3}} = \frac{1.72 \times 10^{-8} \times 0.1}{0.203 \times 10^{-3} \times 20 \times 10^{-3}} = 0.423 \text{ m}\Omega. \quad (36)$$

Since the optimum thickness h_{optn} of the subsequent layers decreases, the dc resistance of the individual layers increases with increasing layer number n .

The total dc winding resistance is a sum of dc winding resistance of each layer

$$R_{wdc} = R_{wdc1} + R_{wdc2} + R_{wdc3} = 0.917 \text{ m}\Omega. \quad (37)$$

Assuming an RMS current of 50 A, the dc and low-frequency power loss in each layer of the inductor is

$$P_{wdc1} = R_{wdc1} I_{rms}^2 = 0.172 \times 50^2 = 0.43 \text{ W}, \quad (38)$$

$$P_{wdc2} = R_{wdc2} I_{rms}^2 = 0.322 \times 50^2 = 0.805 \text{ W}, \quad (39)$$

and

$$P_{wdc3} = R_{wdc3} I_{rms}^2 = 0.423 \times 50^2 = 1.057 \text{ W}. \quad (40)$$

The total dc winding power loss is a sum of dc power loss of each layer

$$\begin{aligned} P_{wdc} &= P_{wdc1} + P_{wdc2} + P_{wdc3} \\ &= 0.43 + 0.805 + 1.057 = 2.292 \text{ W}. \end{aligned} \quad (41)$$

It can be seen that the dc winding power loss of the subsequent layers increases with the layer number. Substituting the optimum layer thickness given by (24) and (26) into (7), the minimum values of the ac-to-dc resistance of n -th layer $F_{Rn(min)}$ were calculated numerically. The results are $F_{R1(min)} = 1.4407$, $F_{R2(min)} = 1.3703$, $F_{R3(min)} = 1.3458$. Hence, the ac resistances in the subsequent layers are

$$\begin{aligned} R_{w1(min)} &= F_{R1(min)} R_{wdc1} = 1.4407 \times 0.172 \times 10^{-3} \\ &= 0.2478 \text{ m}\Omega, \end{aligned} \quad (42)$$

$$\begin{aligned} R_{w2(min)} &= F_{R2(min)} R_{wdc2} = 1.3703 \times 0.322 \times 10^{-3} \\ &= 0.4412 \text{ m}\Omega, \end{aligned} \quad (43)$$

and

$$\begin{aligned} R_{w3(min)} &= F_{R3(min)} R_{wdc3} = 1.3458 \times 0.423 \times 10^{-3} \\ &= 0.5692 \text{ m}\Omega. \end{aligned} \quad (44)$$

The total ac winding resistance of an inductor with the optimum layer thicknesses is

$$\begin{aligned} R_{wmin} &= R_{w1(min)} + R_{w2(min)} + R_{w3(min)} \\ &= 0.2478 + 0.4412 + 1.3458 = 1.2582 \text{ m}\Omega. \end{aligned} \quad (45)$$

Fig. 13 shows the ac winding resistance $R_{wn(min)}$ of each layer and the total ac winding resistance R_{wmin} as functions of frequency f for three-layer winding ($N_l = 3$). The ac power losses in the individual layers for a sinusoidal inductor current of RMS value $I_{rms} = 50 \text{ A}$ are

$$P_{w1(min)} = R_{w1(min)} I_{rms}^2 = 0.2478 \times 50^2 = 0.6195 \text{ W}, \quad (46)$$

$$P_{w2(min)} = R_{w2(min)} I_{rms}^2 = 0.4412 \times 50^2 = 1.103 \text{ W}, \quad (47)$$

$$P_{w3(min)} = R_{w3(min)} I_{rms}^2 = 0.5692 \times 50^2 = 1.423 \text{ W}. \quad (48)$$

It can be seen that the ac power loss in each layer increases with the layer number n .

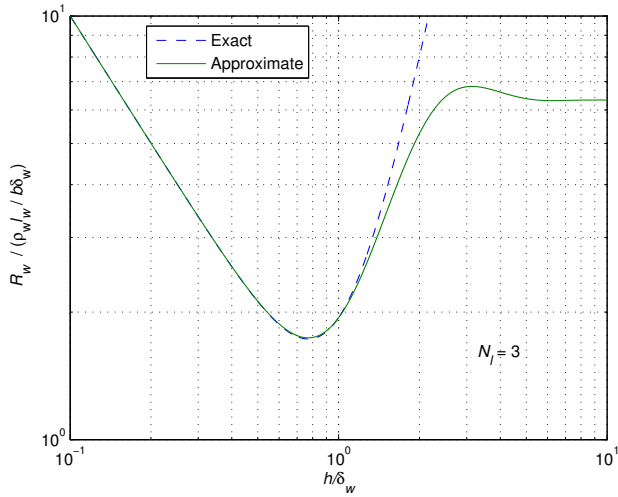


Fig. 14. Exact and approximate plots of $R_w/(\delta_w l_w/b\delta_w)$ as functions of h/δ_w for three-layer inductor $N_l = 3$ for low and medium uniform thickness.

The total minimum ac power loss in the inductor winding is given by

$$\begin{aligned} P_{wmin} &= P_{w1(min)} + P_{w2(min)} + P_{w3(min)} \\ &= 0.6195 + 1.103 + 1.423 = 3.1455 \text{ W}, \end{aligned} \quad (49)$$

which gives the ratio of the ac-to-dc winding resistance and ac-to-dc winding power loss

$$\frac{R_{wmin}}{R_{wdc}} = \frac{P_{wmin}}{P_{wdc}} = \frac{3.1455}{2.292} \approx 1.37. \quad (50)$$

VI. MINIMUM WINDING RESISTANCE FOR INDUCTORS WITH UNIFORM FOIL THICKNESS

For low and medium foil thicknesses, the normalized resistance of the inductor with fixed foil thickness and any number of layers N_l can be approximated by [18]

$$\frac{R_w}{\left(\frac{\rho_w l_w}{b\delta_w}\right)} \approx \frac{1}{\frac{h}{\delta_w}} + \frac{2(N_l^2 - 1)}{17} \left(\frac{h}{\delta_w}\right)^3 \text{ for } \frac{h}{\delta_w} < 1.5, \quad (51)$$

where $l_w = N_l l_T$ is the total foil winding length. Fig. 14 shows exact and approximate plots of $R_w/(\delta_w l_w/b\delta_w)$ as

TABLE II
APROXIMATE OPTIMUM UNIFORM FOIL THICKNESS FOR MULTILAYER INDUCTOR

Layer Number	Approximate
N_l	h_{opt}/δ_w
1	1.5707
2	0.9858
3	0.7714
4	0.6593
5	0.5862
6	0.5334
7	0.4929
8	0.4605
9	0.4338
10	0.4113

functions of h/δ_w for three-layer inductor ($N_l = 3$) with uniform foil thickness for low and medium foil thicknesses. The minimum values of the ac winding resistance R_{wopt} and the winding power loss P_{wopt} of an inductor with uniform foil thickness are determined by taking the derivative of (51) and setting the result to zero

$$\frac{d\left(\frac{R_w}{\frac{\rho_w l_w}{b\delta_w}}\right)}{d\left(\frac{h}{\delta_w}\right)} = \frac{-1}{\left(\frac{h}{\delta_w}\right)^2} + \frac{6(N_l^2 - 1)}{17} \left(\frac{h}{\delta_w}\right)^2 = 0, \quad (52)$$

yielding the optimum value of the uniform foil thickness in the inductor

$$\frac{h_{opt}}{\delta_w} = \frac{1}{\sqrt[4]{\frac{6(N_l^2 - 1)}{17}}} \text{ for } N_l \geq 2. \quad (53)$$

The approximate results of h_{opt}/δ_w , are listed in Table II. For $N_l = 1$, the optimum foil thickness is defined by (24).

In the subsequent analysis, the properties of winding with non-uniform thickness will be compared with those of the winding with uniform thickness. For a three-layer copper inductor ($N_l = 3$) with an uniform foil thickness h and conducting a sinusoidal current at frequency $f = 43$ kHz, the optimum thickness of the bare foil is

$$h_{opt} = 0.7714\delta_w = 0.7741\sqrt{\frac{\rho_w}{\pi f \mu_0}} \approx 0.245 \text{ mm}. \quad (54)$$

The dc and low frequency winding resistance is [18]

$$R_{wdc} = \frac{\rho_c u l_w}{A_{wopt}} = \frac{\rho_c u l_T N_l}{b h_{opt}} = 1.053 \text{ m}\Omega, \quad (55)$$

where A_{wopt} is the cross-sectional area of the foil. Assuming an RMS current of 50 A, the dc and low-frequency power loss in all three layers ($N_l = 3$) of the inductor is given by

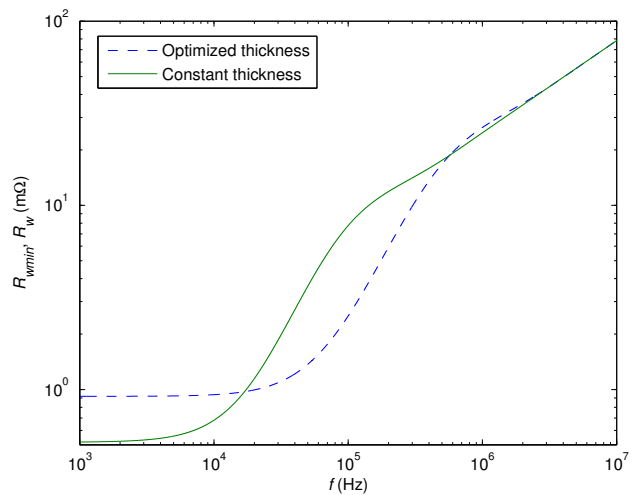


Fig. 15. Plots of R_{wmin} and R_w as functions of frequency f for the inductor with optimized thickness of each layer $h_{opt1} = 0.5$ mm, $h_{opt2} = 0.267$ mm, $h_{opt3} = 0.203$ mm and for the inductor with a constant layer of thickness $h = h_{opt1} = 0.5$ mm.

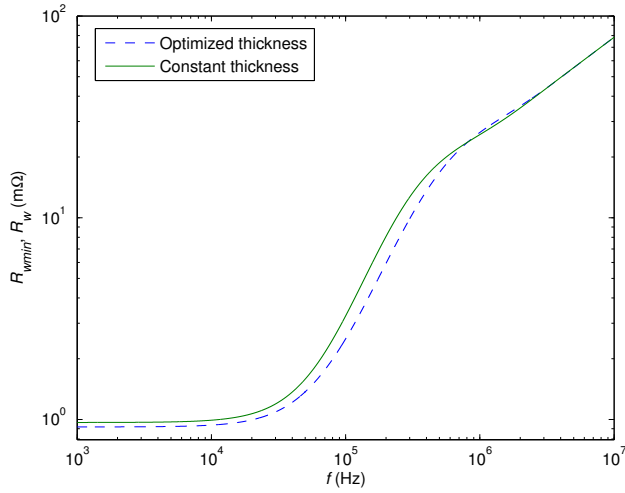


Fig. 16. Plots of R_{wmin} and R_w as functions of frequency f for the inductor with optimized thickness of each layer $h_{opt1} = 0.5$ mm, $h_{opt2} = 0.267$ mm, $h_{opt3} = 0.203$ mm and for the inductor with a constant layer of thickness $h = h_{opt2} = 0.267$ mm.

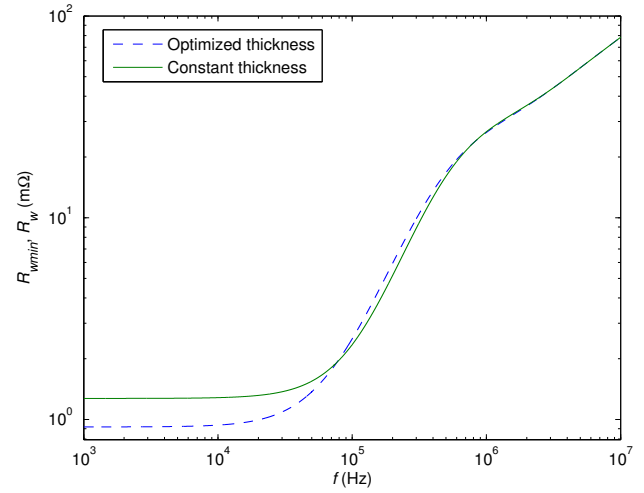


Fig. 17. Plots of R_{wmin} and R_w as functions of frequency f for the inductor with optimized thickness of each layer $h_{opt1} = 0.5$ mm, $h_{opt2} = 0.267$ mm, $h_{opt3} = 0.203$ mm and for the inductor with a constant layer of thickness $h = h_{opt3} = 0.203$ mm.

$$P_{dc} = R_{dc} I_{rms}^2 = 1.053 \times 10^{-3} \times 50^2 = 2.6325 \text{ W.} \quad (56)$$

The ac-to-dc total winding resistance ratio of three-layer inductor with an uniform optimum winding thickness [18] was calculated numerically and is given by

$$F_R = \frac{R_{wopt}}{R_{dc}} = \frac{P_{wopt}}{P_{dc}} = 1.3414. \quad (57)$$

Hence, the optimum ac winding resistance of the inductor with uniform foil thickness is

$$R_{wopt} = F_R R_{dc} = 1.3414 \times 1.053 \times 10^{-3} = 1.4125 \text{ m}\Omega. \quad (58)$$

The total ac winding power loss is

$$P_{wopt} = R_{wopt} I_{rms}^2 = 1.4125 \times 10^{-3} \times 50^2 = 3.5312 \text{ W.} \quad (59)$$

The ratio of the ac winding resistance R_{wopt} of the inductor with the optimum uniform foil thickness to the ac winding resistance R_{wmin} of the inductor with optimum foil thickness for each layer is

$$\epsilon = \frac{R_{wopt}}{R_{wmin}} = \frac{1.4125}{1.2582} = 1.1226. \quad (60)$$

Fig. 15 compares the ac winding resistance R_{wmin} of an inductor with the optimum individual layer thicknesses and the ac winding resistance R_w of an inductor with uniform foil thickness equal to the optimum thickness of the first layer $h = h_{opt1}$ for three layers. It can be seen that for the high-frequency range the ac winding resistance R_{wmin} of the inductor with the optimum individual layer thicknesses is significantly lower than the ac winding resistance R_w of the inductor with a uniform foil thickness. Fig. 16 compares the ac winding resistance R_{wmin} of an inductor with the optimum individual layer thicknesses and the ac winding resistance R_w

of an inductor with an uniform foil thickness equal to the optimum thickness of the second layer $h = h_{opt2}$ for three layers. It can be seen that for the high-frequency range the ac winding resistance R_{wmin} of the inductor with optimized foil thicknesses is approximately equal to the ac winding resistance R_w of the inductor with an uniform foil thickness equal to the optimum thickness of the second layer. Fig. 17 compares the ac winding resistance R_{wmin} of an inductor with the optimum individual layer thicknesses and the ac winding resistance R_w of an inductor with an uniform foil thickness equal to the optimum thickness of the third layer $h = h_{opt3}$ for three layers. Fig. 18 compares the ac winding resistance R_{wmin} of an inductor with the optimum individual layer thicknesses

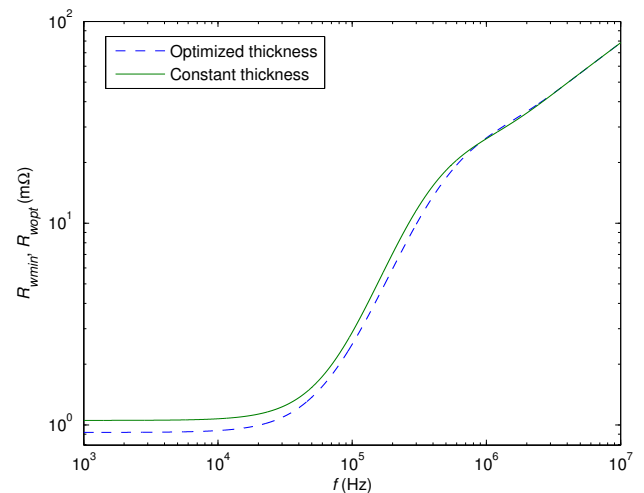


Fig. 18. Plots of R_{wmin} and R_w as functions of frequency f for the inductor with optimized thickness of each layer $h_{opt1} = 0.5$ mm, $h_{opt2} = 0.267$ mm, $h_{opt3} = 0.203$ mm and for the inductor with a constant layer of thickness $h_{opt} = 0.245$ mm for three-layer inductor ($N_l = 3$).

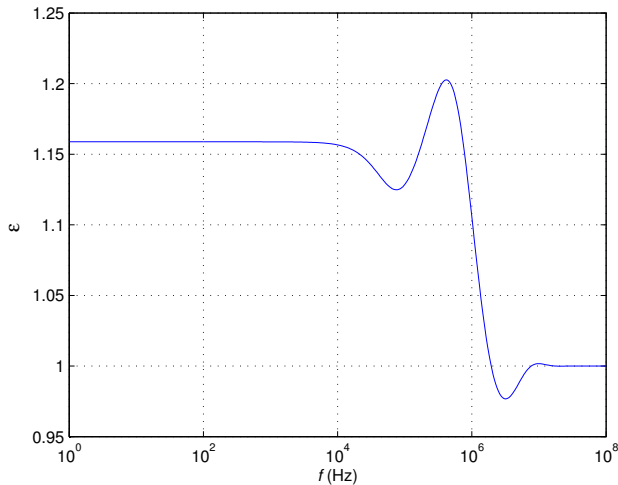


Fig. 19. Ratio of the winding resistance with uniform optimum foil thickness $h_{opt1} = 0.5$ mm, $h_{opt2} = 0.267$ mm, $h_{opt3} = 0.203$ mm to the winding resistance with optimum individual layer thicknesses $h_{opt} = 0.245$ mm for three-layer inductor ($N_l = 3$).

and the ac winding resistance $R_{w_{opt}}$ of an inductor with a uniform optimum foil thickness h_{opt} for three layers. It can be seen that the resistance for inductor with the optimized thickness for each layer is lower than that of the inductor with the uniform optimum thickness. Fig. 19 shows the ratio of the ac winding resistance $R_{w_{opt}}$ with uniform optimum foil thickness to the ac winding resistance $R_{w_{min}}$ with the optimum individual layer thicknesses.

It can be seen that the resistance of the inductor with the optimum uniform foil thickness for the low-frequency range is 13% higher than that of the inductor with the optimized thickness of each layer. In the medium-frequency range, the resistance of uniform inductor winding thickness increases. At a frequency of 200 kHz, the winding resistance of the inductor with the optimum uniform thickness is 21.8% greater than the winding resistance of the inductor with the optimum foil thickness of individual layers. However, in the high-frequency range, the winding resistances of both inductors are the same.

The inductance of the foil wound inductor is expressed by

$$L = \frac{\mu_{rc}\mu_0 A_c N_l^2}{b}$$

$$= \frac{1800 \times 4\pi \times 10^{-7} \times 4 \times 10^{-4} \times 3^2}{2 \times 10^{-2}} \approx 407 \mu\text{H}, \quad (61)$$

where $b = 2$ cm, $\mu_{rc} = 1800$ is the core permeability, $N_l = 3$ is the number of layers, and $A_c = 4$ cm² is the cross-sectional area of the core.

VII. CONCLUSIONS

The equation for the winding resistance of individual layers for inductors made of foil conductor has been analysed and illustrated. This equation has been approximated to derive an expression for the optimum thickness of individual layers. The comparison of winding resistances at various values of foil thickness has been presented. It has been shown that the

minimum value of the winding resistance of each individual layer at a fixed frequency occurs at different values of the normalized layer thickness h_{optn}/δ_w . The optimum normalized layer thickness h_{optn}/δ_w decreases with increasing layer number n . In addition, the resistance of each layer appreciably increases as the layer number n increases from the innermost to the outermost layer. Moreover, the approximated equation for low-frequency resistance of inductors with a uniform foil thickness has been given.

The optimum normalized value of the uniform foil thickness has been derived. It has been shown that the winding resistance of the inductor with an optimum uniform foil thickness for low-frequency range is 13% higher than that of the inductor with an optimized thickness of each layer.

In the medium-frequency range, the ratio of the winding resistance with a uniform optimum foil thickness to the winding resistance with the optimum thickness of each individual layer first increases, reaches a maximum value, and then rapidly decreases with frequency. At a frequency of 200 kHz, the winding resistance of uniform optimum foil thickness was 21.8% greater than the winding resistance of the inductor with the optimum foil thickness of each layer, in the given example. For the high-frequency range, the winding resistances of both inductors were identical. High-quality power inductors are used in high-frequency applications, such as pulse-width-modulated (PWM) DC-to-DC power converters [14], [19], [20], resonant DC-to-DC power converters [4], radio-frequency power amplifiers [15]-[17], and LC oscillators [1].

REFERENCES

- [1] A. Aminian and M. Kazimierczuk, *Electronic Devices. A Design Approach*. Upper Saddle, NJ: Prentice Hall, 2004.
- [2] M. Bartoli, N. Noferi, A. Reatti, and M. K. Kazimierczuk, "Modeling winding losses in high-frequency power inductors," *Journal of Circuits, Systems and Computers*, vol. 5, no. 4, pp. 607-626, December 1995.
- [3] E. Bennett and S. C. Larsen, "Effective resistance to alternating currents of multilayer windings," *Trans. Amer. Inst. Elect. Eng.*, vol. 59, pp. 1010-1017, 1940.
- [4] N. Das and M. K. Kazimierczuk, "An overview of technical challenges in the design of current transformers," in *Electrical Manufacturing Conference*, Indianapolis, IN, USA, October 24-26 2005.
- [5] P. J. Dowell, "Effects of eddy currents in transformer winding," *Proc. IEE*, vol. 113, no. 8, pp. 1387-1394, August 1966.
- [6] M. J. Hole and L. C. Appel, "Stray capacitance of two-layer air-cored inductor," *IEE Proceedings, Part G, Circuits, Devices and Systems*, vol. 152, no. 6, pp. 565-572, December 2005.
- [7] M. K. Kazimierczuk, *Pulse-Width Modulated DC-DC Power Converters*. Chichester, UK: John Wiley & Sons, 2008.
- [8] —, *RF Power Amplifiers*. Chichester, UK: John Wiley & Sons, 2008.
- [9] —, *High-Frequency Magnetic Components*. Chichester, UK: John Wiley & Sons, November 2009.
- [10] M. K. Kazimierczuk and D. Czarkowski, *Resonant Power Converters*. New York, NY, USA: John Wiley & Sons, 1995.
- [11] M. K. Kazimierczuk and H. Sekiya, "Design of ac resonant inductors using area product method," in *IEEE Energy Conversion Conference and Exhibition*, San Jose, CA, USA, September 20-24 2009, pp. 994-1001.
- [12] N. H. Kutkut, "A simple technique to evaluate winding losses including two-dimensional edge effect," *IEEE Transactions on Power Electronics*, vol. 13, no. 5, pp. 950-958, September 1998.
- [13] N. H. Kutkut and D. M. Divan, "Optimal air-gap design in high-frequency foil windings," *IEEE Transaction on Power Electronics*, vol. 13, no. 5, pp. 942-949, September 1998.
- [14] D. Murthy-Bellur and M. K. Kazimierczuk, "Harmonic winding loss in buck dc-dc converter for discontinuous conduction mode," *IET Power Electron.*, vol. 3, no. 5, pp. 740-754, 2010.

- [15] —, “Winding losses caused by harmonics in high-frequency flyback transformers for pulse-width modulated dc-dc converters in discontinuous conduction mode,” *IET Power Electron.*, vol. 3, no. 5, pp. 804–817, 2010.
- [16] D. C. Pentz and I. W. Hofsajer, “Improved AC-resistance of multiple foil winding by varying of thickness of successive layers,” *COMPEL: The International Journal for Computation and Mathematics in Electrical and Electronic Engineering*, vol. 27, no. 1, pp. 181–195, 2008.
- [17] M. P. Perry, “Multiple layer series connected winding design for minimum losses,” *IEEE Transactions on Power Apparatus and Systems*, vol. PAS-98, no. 1, pp. 116–123, January/February 1979.
- [18] A. Reatti and M. K. Kazimierczuk, “Comparison of various methods for calculating the ac resistance of inductors,” *IEEE Transactions on Magnetics*, vol. 37, no. 3, pp. 1512–1518, May 2002.
- [19] P. Scoggins, “A guide to design copper-foil inductors,” *Power Electronics Technology*, pp. 30–34, July 2007.
- [20] H. Sekiya and M. K. Kazimierczuk, “Design of RF-choke inductors using core geometry coefficient,” in *Proc. of the Electrical Manufacturing and Coil Winding Conf.*, Nashville, TN, USA, September 29–October 1 2009.